Masubuchi *et al. Clinical Epigenetics* (2026) 18:38
https://doi.org/10.1186/s13148-026-02065-5

Clinical Epigenetics

RESEARCH Open Access

Methylation profile characteristics in the *H19/IGF2*:IG-DMR revealed by long-read sequencing analysis in patients with Beckwith-Wiedemann syndrome having defects in the OCT4/SOX2 binding site

Hayate Masubuchi[1,2], Tatsuki Urakawa[1,3], Rika Kosaki[4], Riki Nishimura[5,6], Yasunori Wada[7], Sumito Dateki[3], Hideaki Yagasaki[8], Reiko Kagawa[9], Yutaka Nishimura[10], Hidenobu Soejima[11], Tsutomu Ogata[12,13], Maki Fukami[1] and Masayo Kagami[1*]

Abstract

Background Beckwith-Wiedemann syndrome (BWS) is an imprinting disorder with characteristic clinical features such as overgrowth and macroglossia. Hypermethylation of the *H19/IGF2*:IG-differentially methylated region (*H19*-DMR) is identified in 5% of BWS patients. Although defects in the OCT4/SOX2 binding sites (OBS) on the maternal allele have been reported in patients with hypermethylated *H19*-DMR, the precise methylation patterns in patients with OBS abnormalities remain elusive. Nanopore long-read sequencing (LRS) obtains sequence reads 10–100 kb long together with single-molecule DNA modifications, such as 5-methylcytosines. Furthermore, LRS can separate reads into haplotypes 1 and 2 based on information from single-nucleotide variants and indels on reads. Here, we conducted LRS to elucidate the abnormal hypermethylation patterns of the *H19*-DMR in BWS patients with and without OBS abnormalities and evaluate the differences between mothers and their offspring in familial cases with OBS abnormalities.

Results We included 14 sporadic patients and four familial patients from two families with BWS showing hypermethylation of the *H19*-DMR. Amplicon sequencing for the *H19*-DMR detected OBS abnormalities in four (28.6%) sporadic cases (three point mutations, one 21-bp microdeletion overlapping OBS), an OBS point mutation in family A, and a 2.6 kb deletion involving OBS in family B. Subsequently, we conducted targeted LRS and examined methylation indexes for 247 CpGs in the *H19*-DMR in three sporadic patients with OBS abnormalities, two sporadic patients without OBS abnormalities, and all familial patients with OBS abnormalities. In patients with point mutations and a 21-bp microdeletion affecting a single base in OBS, CpGs in the *H19*-DMR had obvious hypermethylation in the vicinity of OBS and mild-to-moderate hypermethylation with increased distance from OBS; however, in patients

*Correspondence:
Masayo Kagami
kagami-ms@ncchd.go.jp

Full list of author information is available at the end of the article

with deletions including OBS, CpGs had moderate hypermethylation in the entire *H19*-DMR. In families A and B, methylation levels were higher in offspring than in their mothers.

Conclusion Because 28.6% of sporadic patients had OBS abnormalities, genetic examination for OBS should be considered in BWS patients with hypermethylated *H19*-DMR. LRS analysis for the *H19*-DMR revealed differences in methylation patterns between patients with and without OBS abnormalities and the methylation levels of each CpG between mothers and their offspring in families with OBS abnormalities.

Keywords Beckwith-Wiedemann syndrome, *H19/IGF2*:IG-DMR, OCT4/SOX2 binding site, Long-read sequencing, Methylation analysis

Background

Beckwith-Wiedemann syndrome (BWS; OMIM #130,650) is an imprinting disorder characterized by distinctive clinical features, such as overgrowth, macroglossia, and abdominal wall defects [1, 2]. The BWS-responsible 11p15.5 imprinted region has two imprinting centers, the *H19/IGF2*:IG-differentially methylated region (*H19*-DMR), so-called imprinting center 1, and the *KCNQ1OT1*:TSS-DMR (*Kv*-DMR), so-called imprinting center 2 [3]. BWS is caused by abnormal expression of the imprinted genes at the 11p15.5 imprinted region, increased expression of the paternally expressed *IGF2* gene, and/or decreased expression of the maternally expressed *CDKN1C* gene [4]. Hypomethylation of the *Kv*-DMR observed in 50% of patients with BWS results in decreased *CDKN1C* expression, and hypermethylation of the *H19*-DMR identified in 5% of patients with BWS causes increased *IGF2* expression [5, 6]. Recently, the concept of the Beckwith-Wiedemann spectrum (BWSp) and the BWSp score as a clinical scoring system have been proposed [1]. The BWSp score consists of basic features with two points and suggestive features with one point [1]. Patients with a score of four or more on the BWSp are clinically diagnosed with BWS, and those with a score of two or more are recommended to undergo genetic testing for BWS [1].

The CpGs in the *H19*-DMR, located approximately 6 kb within the 11p15.5 imprinted region, are unmethylated on the maternally inherited allele and methylated on the paternally inherited allele. Gain of methylation at the *H19*-DMR on the maternal allele leads to biallelic *IGF2* expression and silencing of *H19* and causes BWS phenotype. The OCT4/SOX2 binding sites (OBS) within the *H19*-DMR function to maintain the unmethylated *H19*-DMR on the maternal allele [7]. The *H19*-DMR defined by Monk et al. [8] does not include OBS0, but OBS0 is in the vicinity of the *H19*-DMR, whereas OBS1 and OBS2 are positioned within the *H19*-DMR [9]. Mutations or deletions involving the OBS1 on the maternal allele cause hypermethylation of the *H19*-DMR due to failure of protection from genome-wide de novo methylation after fertilization [9, 10]. In a previous study, approximately 20% of BWS patients with hypermethylated *H19*-DMR had OBS abnormalities [10]. However, the precise methylation pattern in patients with defects of the OBS remains elusive.

Long-read sequencing (LRS) analysis, released by Oxford Nanopore Technologies (ONT), obtains sequence reads 10–100 kb long together with single-molecule DNA modifications, such as 5-methylcytosines (5-mC), by measuring changes in the electrical signal generated when DNA strands pass through a biological pore [11, 12]. Furthermore, based on the information of single-nucleotide variants and indels on reads, LRS can separate the reads into haplotypes 1 and 2. A previous study showed that 12 or more reads are needed to obtain reliable methylation indexes with a probability of more than 90% using LRS [13]. Targeted-LRS (T-LRS) using adaptive sampling enriches 0.1%–10% of the whole-genome region and achieves 5–10 times greater depth than whole-genome LRS [14]. We believe that LRS is a suitable method for accessing the contiguous methylation levels of CpGs across the entire *H19*-DMR. Here, we examined OBS abnormalities in patients with BWS showing hypermethylation of the *H19*-DMR using amplicon sequencing, conducted sequence and methylation analyses using T-LRS in patients with OBS abnormalities and patients without OBS abnormalities, and revealed the methylation patterns in patients with OBS abnormalities and methylation levels of each CpG between mothers and their offspring in families with OBS abnormalities.

Results

The study flow is shown in Fig. 1.

Identification of the patients with hypermethylation of the *H19*-DMR

We conducted methylation analysis using methylation-specific multiplex ligation-dependent probe amplification (MS-MLPA) [15] and/or pyrosequencing as previously reported [16–18] for the *H19*-DMR and *Kv*-DMR in 233 patients suspected of having BWS and detected 18 patients with hypermethylation of the *H19*-DMR alone. Of these patients, 14 were sporadic cases, and four were familial cases (Fig. 1, Fig. S1, and Table 1). As shown in Fig. S1, sporadic Pt. 4 and Family B, comprising Pt. 7

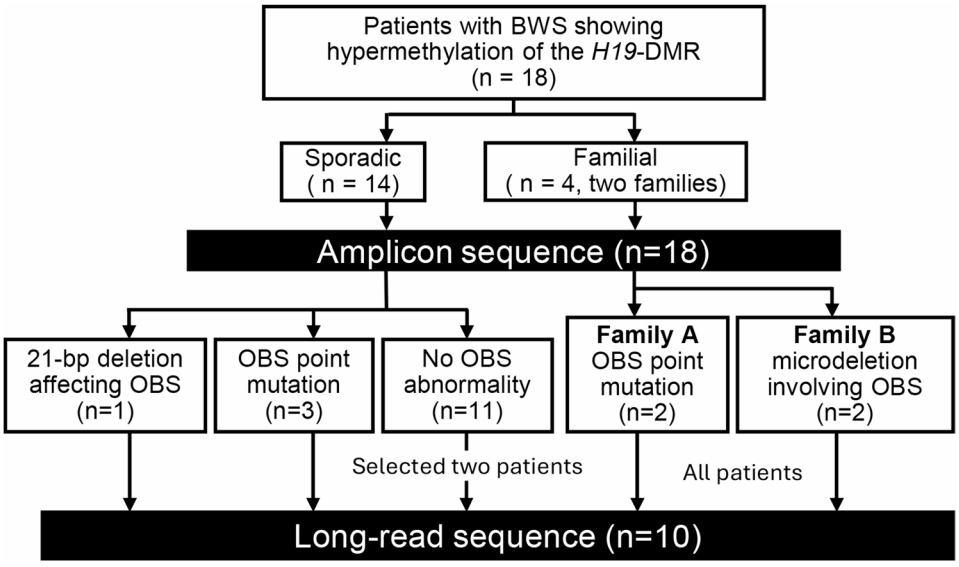

Fig. 1 Study flowchart. BWS, Beckwith-Wiedemann syndrome; DMR, differentially methylated region; *H19*-DMR, *H19/IGF2*:IG-DMR; OBS, OCT4/SOX2 binding site

(mother) and 8 (offspring), had a probe with a decreased copy number in the *H19*-DMR.

Amplicon sequence analysis for the *H19*-DMR and identification of OBS abnormalities

We conducted amplicon sequencing for the *H19*-DMR, including three OBS with the next-generation sequencer in 18 patients (14 sporadic patients and 4 familial patients) as previously reported [19] and detected point mutations, a 21-bp microdeletion affecting a single base in OBS, and microdeletions including OBS in four out of 14 sporadic patients and four patients from two families. Pt. 1 and 2 had the previously reported same point mutation (chr11:2,001,789 A > G, hg38) in OBS [10, 20], and Pt. 3 had a novel point mutation (chr11:2,001,784 T > A) in OBS (Fig. 2A). We confirmed these mutations in OBS by Sanger sequencing (Fig. 2B). Subsequently, we conducted Sanger sequencing on the family members, although we could not obtain samples from the family members of Pt. 1. We identified the same mutations in mothers of Pt. 2 and Pt. 3, but not in the grandfathers or grandmothers of both patients. To clarify the parental origin of OBS mutations in their mothers, we conducted Sanger sequencing using genomic DNA of the mothers treated with methylation-sensitive restriction enzymes (MSRE) as previously reported [21] and confirmed the mutations in both mothers on the paternal allele (Fig. S2). Pt. 4 had a 21-bp deletion affecting a single base in OBS (chr11:2,001,763–2,001,783) (Fig. 2C). Sanger sequencing revealed that the mother also had the same 21-bp deletion (Fig. S2). Family A, consisting of Pt. 5 (mother) and Pt. 6 (offspring), had previously revealed a point mutation (chr11:2,001,788 C > T) in OBS (Fig. 2A and D) [9, 22]. Family B, consisting of Pt. 7 (mother) and 8 (offspring), had a microdeletion involving OBS (chr11: 2,001,595–2,004,249) (Fig. 2E).

Clinical characteristics of the patients

The clinical features of patients with and without OBS abnormalities are shown in Table 2. We were unable to obtain clinical information in three patients without OBS abnormalities. All patients with OBS abnormalities had a score of four or more on the BWSp and showed macroglossia and large birth weight (≥ 2 standard deviations [SD]). Omphalocele, hyperinsulinism, transient hypoglycemia, and embryonic tumors including Wilms tumor, were not observed in any patients with OBS abnormalities. In family A, the mother and offspring had four and five points, respectively, and in family B, the mother and offspring had six and five points, respectively. Lateralized overgrowth was shown only in family B.

Definition of the normal range of CpGs in the *H19*-DMR in T-LRS

We conducted LRS analysis in seven normal controls and determined the normal range of MIs for all CpGs in the *H19*-DMR. We defined the normal range of MI for each CpG as |MI| < 3 SD in seven healthy controls (Table S1). We designed targeted regions for the *H19*-DMR and other DMRs using adaptive sampling based on previous studies [8, 23], which comprised 1.2% of the whole genome (Table S2). The *H19*-DMR included 247 CpGs. We calculated MI for a CpG with 12 or more read counts in each control, following a previous study [13]. Figure 3 shows the normal range of the MIs in the *H19*-DMR determined by LRS analysis. The normal range of MIs in CpGs within the *H19*-DMR were typically around 0.5

Table 1 Results of the methylation analysis using pyrosequencing in patients with hypermethylation of the *H19*-DMR

		Position	P1	P2	P3	P4	P5	P6	P7	P8	P9	P10	P11	P12	P13
Normal range		**Min**	**48**	**45**	**49**	**43**	**46**	**36**	**57**	**54**	**57**	**55**	**52**	**56**	**43**
		Max	**54**	**57**	**58**	**51**	**54**	**46**	**63**	**60**	**65**	**61**	**57**	**64**	**49**
Pt	**Sp or Fam**	**OBS abnormality**													
Pt. 1	Sp	Mut	**82**	**86**	**92**	**80**	**80**	**69**	**81**	**78**	**82**	**79**	**76**	**82**	**61**
Pt. 2	Sp	Mut	**78**	**85**	**78**	**53**	**76**	**56**	**69**	**63**	**77**	**67**	**64**	**76**	44
Pt. 3	Sp	Mut	**86**	**92**	**98**	**88**	**84**	**71**	**93**	**88**	**98**	**91**	**89**	**94**	**66**
Pt. 4	Sp	Del	**83**	**91**	**95**	**88**	**83**	**67**	**73**	**68**	**76**	**70**	**68**	**74**	**53**
Pt. 5	Fam (Mo)	Mut	**84**	**94**	**97**	**89**	**87**	**72**	**76**	**72**	**85**	**76**	**73**	**81**	**50**
Pt. 6	Fam (Off)	Mut	**84**	**100**	**100**	**88**	**82**	**68**	**84**	**79**	**89**	**82**	**79**	**86**	**60**
Pt. 7	Fam (Mo)	Del	**85**	**95**	**97**	**85**	**87**	**75**	**67**	**61**	**73**	**64**	**62**	**68**	44
Pt. 8	Fam (Off)	Del	**84**	**96**	**96**	**71**	**83**	**69**	**75**	**71**	**78**	**73**	**71**	**79**	**56**
Pt. 9	Sp	No	**87**	**87**	**92**	**87**	**84**	**74**	**99**	**92**	**97**	**94**	**91**	**98**	**73**
Pt. 10	Sp	No	**91**	**99**	**99**	**92**	**84**	**76**	**96**	**83**	**100**	**93**	**90**	**100**	**69**
Pt. 11	Sp	No	**67**	**71**	**77**	**67**	**68**	**56**	**82**	**78**	**90**	**82**	**78**	**87**	**58**
Pt. 12	Sp	No	**64**	**64**	**70**	**61**	**61**	**51**	**74**	**72**	**76**	**71**	**68**	**74**	**57**
Pt. 13	Sp	No	**86**	**87**	**90**	**85**	**86**	**78**	**92**	**87**	**91**	**88**	**85**	**93**	**71**
Pt. 14	Sp	No	**73**	**77**	**78**	**70**	**72**	**62**	**79**	**76**	**81**	**77**	**74**	**80**	**61**
Pt. 15	Sp	No	**75**	**84**	**81**	**73**	**76**	**65**	**83**	**79**	**85**	**80**	**77**	**86**	**63**
Pt. 16	Sp	No	**90**	**99**	**96**	**94**	**88**	**79**	**95**	**88**	**99**	**94**	**94**	**99**	**74**
Pt. 17	Sp	No	**68**	**74**	**75**	**66**	**66**	**55**	**80**	**76**	**87**	**80**	**77**	**83**	**56**
Pt. 18	Sp	No	**59**	**61**	**65**	**57**	**60**	**48**	**100**	**93**	**98**	**94**	**93**	**100**	**73**

DMR, differentially methylated region; *H19*-DMR, *H19/IGF2*:IG-DMR; OBS, OCT4/SOX2 binding site; P, position; Pt., patient; Max, maximum of normal range; Min, minimum of normal range; Sp, sporadic; Fam, Familial; Mo, mother; Off, offspring; Mut, point mutation; Del, microdeletion. Bold numbers show the abnormally hypermethylated

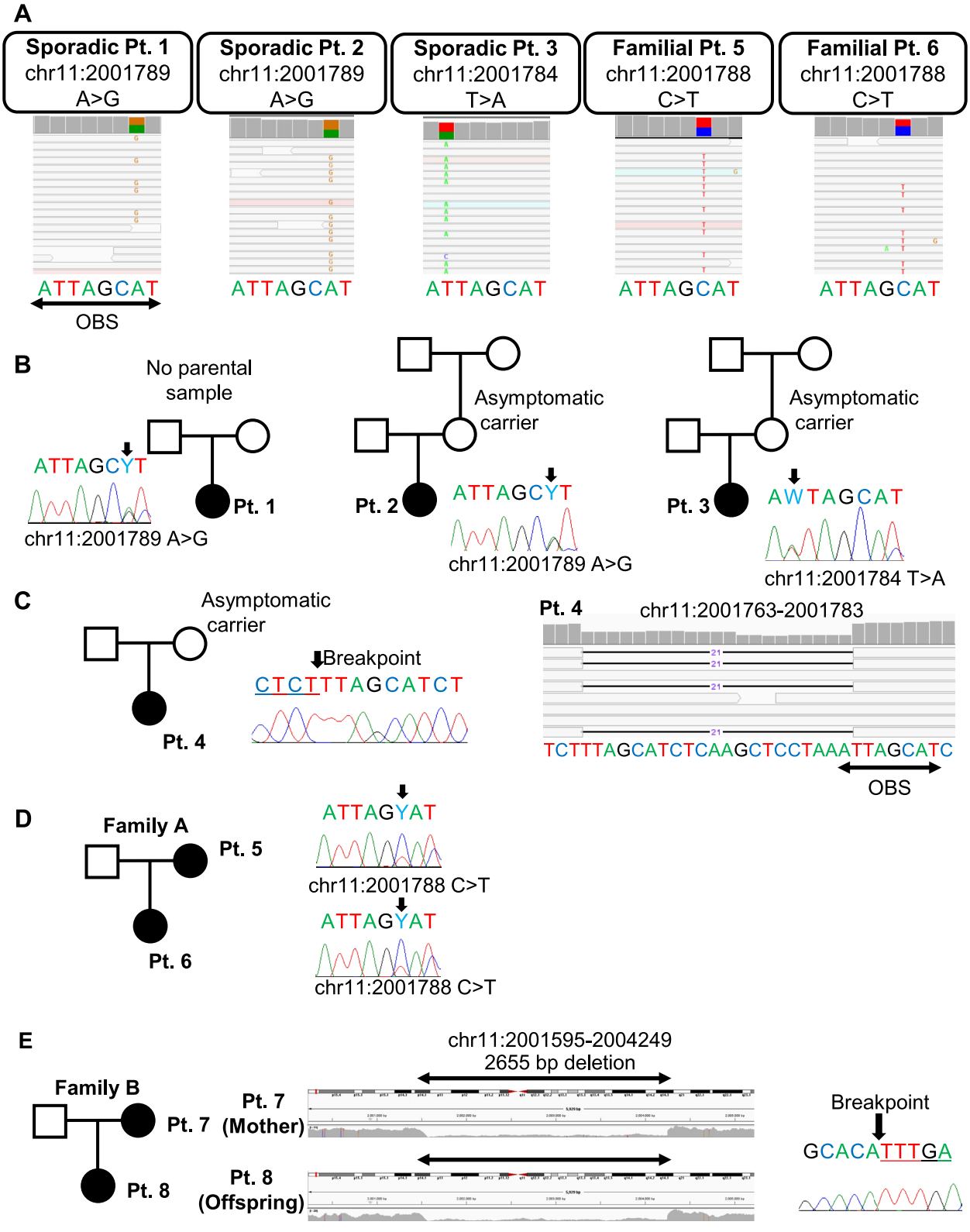

Fig. 2 The results of amplicon sequencing and Sanger sequencing for OBS in patients with defects of OBS and their family members. **A** The results of amplicon sequencing for OBS in patients with point mutations. **B** The results of Sanger sequencing in sporadic patients with OBS point mutations. **C** The results of amplicon sequencing and Sanger sequencing for OBS in patient 4 with a 21-bp deletion. **D** The results of Sanger sequencing for an OBS point mutation in Family A and E Screenshot from IGV for the deleted region involving OBS in Family B and the results of Sanger sequencing for the breakpoint. OBS, OCT4/SOX2 binding sites; Pt, patient, IGV, Integrative Genomics Viewer

Table 2 Clinical findings in patients with BWS caused by hypermethylation of the *H19*-DMR

	Sp. Pt. with OBS abnormalities										
	Point mutation			Micro-deletion	Family A		Family B		Total	Pt. without OBS abnormalities	*P* value[b]
	Pt. 1	Pt. 2	Pt. 3	Pt. 4	Pt. 5	Pt. 6	Pt. 7	Pt. 8	*n* = 8	*n* = 7	
Karyotype (46,XX vs 46,XY)	46,XY	46,XX	46,XX	46,XX	46,XX	46,XY	46,XX	46,XY	5:3	4:3	–
Sex	M	F	F	F	F	M	F	M			–
Present age (years)	5	11	5	12	31	2	28	8	12 (2 to 31)	8 (6 to 12)	–
GA (weeks)	35	38	37	37	36	40	38	39	37.5 (35 to 40)	36 (26 to 38)	0.30
Birth process (C/S vs V)	C/S	V	V	V	V	V	V	V	1:7	5:1	0.01
BL (SDS)[a]	3.8	2.0	1.2	2.3	4.0	5.1	1.0	2.1	2.1 (1.0 to 5.1)	1.9 (1.2 to 4.2)	0.60
BW (SDS)[a]	6.6	2.9	2.5	4.2	5.6	2.0	2.5	2.7	2.8 (2.0 to 6.6)	3.6 (1.8 to 5.6)	0.65
BH (SDS)[a]	0.4	0.7	0.9	0.1	1.1	0.0	U	1.3	0.7 (0.0 to 1.3)	1.0 (0.0 to 2.3)	0.43
BWSp score	8	4	5	7	4	5	6	5	5 (4 to 8)	5 (3 to 6)	0.23
Macroglossia	+	+	+	+	+	+	+	+	8/8	7/7	–
Omphalocele	–	–	–	–	–	–	–	–	0/8	0/7	–
Lateralized overgrowth	+	–	–	–	–	–	+	+	3/8	1/7	0.44
Hyperinsulinism	–	–	–	U	–	–	–	–	0/7	0/7	–
Wilms tumor	–	–	–	–	–	–	–	–	0/8	0/7	–
Abdominal wall defects	–	–	–	–	+	+	+	–	3/8	4/7	0.78
Facial hemangioma	+	–	–	–	–	–	–	–	1/8	0/7	0.21
Polyhydramnios	+	U	–	+	–	–	–	–	2/7	1/7	0.60
Large birth weight	+	+	+	+	+	+	+	+	8/8	4/7	0.04
Ear creases	–	+	+	+	–	–	–	–	3/8	1/7	0.88
Organomegaly	+	–	+	+	–	+	–	–	4/8	4/7	0.45
Embryonal tumors	–	–	–	–	–	–	–	–	0/8	0/7	–
Transient hypoglycemia	–	–	–	+	–	–	–	–	1/8	0/7	0.25

BWS, Beckwith-Wiedemann syndrome; BWSp score, Beckwith-Wiedemann spectrum clinical score; Sp., sporadic; GA, gestational age; Pt., patient, BL, birth length; BW, birth weight; BH, birth head circumference; SDS, standard deviation score; M, male; F, female; U, unknown; C/S, cesarean section; V, vaginal

[a]SDS of the gestational age-matched and sex-matched Japanese reference data (http://jspe.umin.jp/medical/keisan.html)

[b]The Mann–Whitney *U* test was used for finding the statistically significant difference of GA, BL, BW, BH, and BWSp score. Fisher's exact test was used for analysis of the birth process and other BWS symptoms

(completely differentially methylated) in certain regions; however, in other regions, MIs in CpGs were over 0.8, as previously reported [24, 25]. Most CpGs set MS-MLPA probes were completely differentially methylated. Figure 4A shows the results of the methylation analysis using LRS on Integrative Genomics Viewer (IGV) in a normal control. Based on the methylation pattern in the *H19*-DMR, methylated on the paternally inherited allele and unmethylated on the maternally inherited allele, the upper haplotype was inherited from the father, and the lower haplotype was inherited from the mother.

T-LRS analysis in patients with BWS

We conducted T-LRS for two sporadic cases with an OBS point mutation (Pt. 1 and 3), one sporadic case with 21-bp deletion affecting OBS (Pt. 4), four family cases from two families with OBS abnormalities (Pt. 5–8), and two sporadic cases without OBS abnormalities (Pt. 9 and 10). Because Pt. 2 and 3 had the same point mutation previously reported (chr11:2,001,784 T > A) and only Pt. 3 had sufficient DNA sample volume for LRS analysis, we conducted LRS analysis only in Pt. 3. We calculated MIs for CpGs within the *H19*-DMR and evaluated methylation patterns and levels by comparing patients with and without OBS abnormalities, as well as comparing mothers and offspring who shared the same OBS abnormalities within the same family. To obtain 12 or more reads for each CpG, we used two or three MinION flow cells and a half PromethION flow cell for T-LRS in Pt. 5, 6, 7, and 8 and a single PromethION flow cell for T-LRS in Pt. 1, 3, 4, 9, and 10, respectively. Mean coverage of 247 CpGs in the *H19*-DMR were 24.3 in Pt. 1, 24.8 in Pt. 3, 17.4 in Pt. 4, 26.5 in Pt. 5, 22.7 in Pt. 6, 19.7 in Pt. 7, 13.8 in Pt. 8, 25.6 in Pt. 9, and 43.8 in Pt. 10, and the read

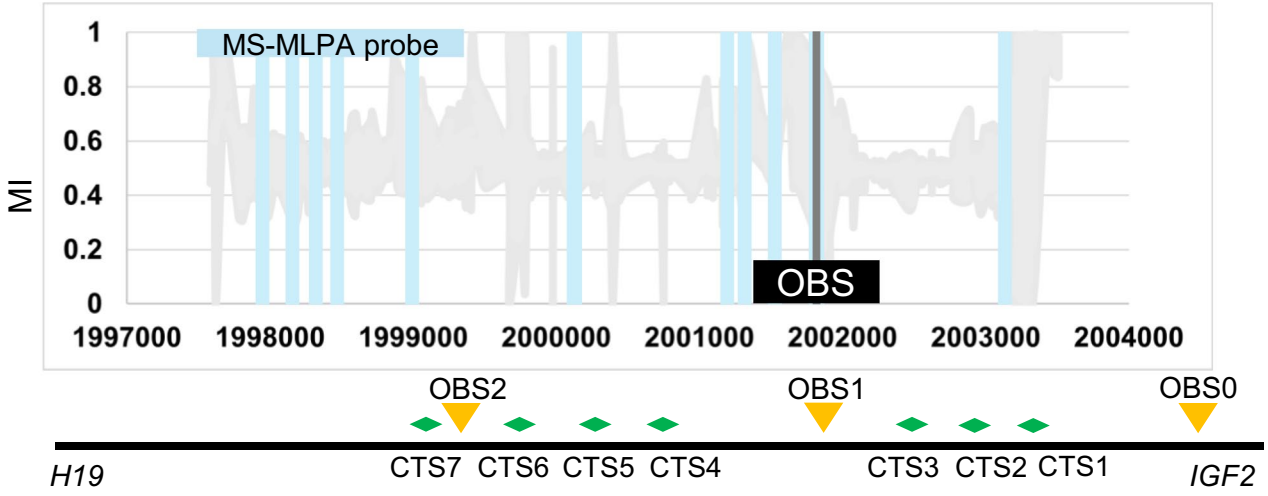

Fig. 3 The normal range of MIs in the *H19*-DMR. The gray background shows the normal range of MIs in CpGs. The light blue bar indicates the probe location examined by MS-MLPA. The yellow triangle and green diamond indicate OBS and CTS, respectively. The sequence reads were aligned for GRCh38. The location of the OBS and the CTS are shown below. MIs, methylation indexes; *H19*-DMR, *H19/IGF2*:IG-DMR; IG, intergenic; DMR, differentially methylated region; MS-MLPA, methylation-specific multiple ligation-dependent probe amplification; OBS, OCT4/SOX2 binding site; CTS, CTCF target site

counts in each CpG in each patient are shown in Table S3. LRS also showed OBS abnormalities in patients 1, 3, 4, 5, 6, 7, and 8 (Fig. 4B).

Subsequently, to evaluate the methylation pattern of the *H19*-DMR in patients with various OBS abnormalities and without OBS abnormalities, we plotted MIs in all CpGs within the *H19*-DMR (Fig. 5). In Pt. 1, 3, 5, and 6 with OBS point mutations, CpGs showed obvious hypermethylation in the locus near the OBS and mild-to-moderate hypermethylation in the locus away from the OBS. In Pt. 4 with a 21-bp deletion affecting a single base in OBS, the methylation pattern was close to that observed in patients with point mutations (Fig. 5). In Pt. 7 and 8 with a microdeletion including OBS, CpGs consistently exhibited moderate hypermethylation in the whole *H19*-DMR. On the other hand, in patients without OBS abnormalities, CpGs showed extreme hypermethylation across the *H19*-DMR (Fig. 5).

Next, we compared methylation levels of CpGs between the mother and the offspring with the same OBS abnormality in each family. In family A, the offspring (Pt. 6) had higher abnormal hypermethylation than the mother (Pt. 5) in most CpGs in the *H19*-DMR (Fig. 5). In Family B, the offspring (Pt. 8) also showed higher abnormal hypermethylation than the mother (Pt. 7) in most CpGs in the *H19*-DMR (Fig. 5). We evaluated the difference in MIs between the mothers and their offspring (ΔMI) (Fig. S3). In both families A and B, ΔMI increased away from the OBS (Fig. S3).

Discussion

We identified OBS abnormalities in four sporadic patients and four patients from two families of 18 patients with BWS showing hypermethylation of the *H19*-DMR. Subsequently, we defined the normal methylation levels of the continuous 247 CpGs in the *H19*-DMR using T-LRS in seven control samples, examined MIs of 247 CpGs within the *H19*-DMR using T-LRS, and showed the characteristics of the methylation patterns in patients with and without OBS abnormalities and differences of the methylation levels in CpGs between mother and offspring in each family with OBS abnormality.

In our study, four (28.5%) out of 14 sporadic patients with BWS had OBS abnormalities. Of them, Pt. 3 and 4 had a novel point mutation (chr11:2,001,784 T > A) and a 21-bp deletion (chr11:2,001,763–2,001,783) on the maternal allele, respectively. The methylation patterns in Pt. 3 and 4 were similar to those in other patients with OBS point mutations (Pt. 1, 5, and 6), which were obvious hypermethylation in CpGs near the OBS and mild-to-moderate hypermethylation in CpGs away from the OBS. In addition, the mothers of Pt. 3 and 4 without BWS phenotype also had the same mutation and a 21-bp microdeletion identified in their children on the paternal allele, respectively. These findings suggest the pathogenicity of this novel point mutation and a 21-bp deletion affecting OBS and leading to BWS. Abi Habib et al. also reported OBS abnormalities in 10 (19.2%) of 52 patients with BWS showing hypermethylation of the *H19*-DMR [10]. Because female patients with OBS abnormalities have a 50% recurrence rate for BWS, sequencing analysis for OBS in patients with hypermethylation of the *H19*-DMR should be considered.

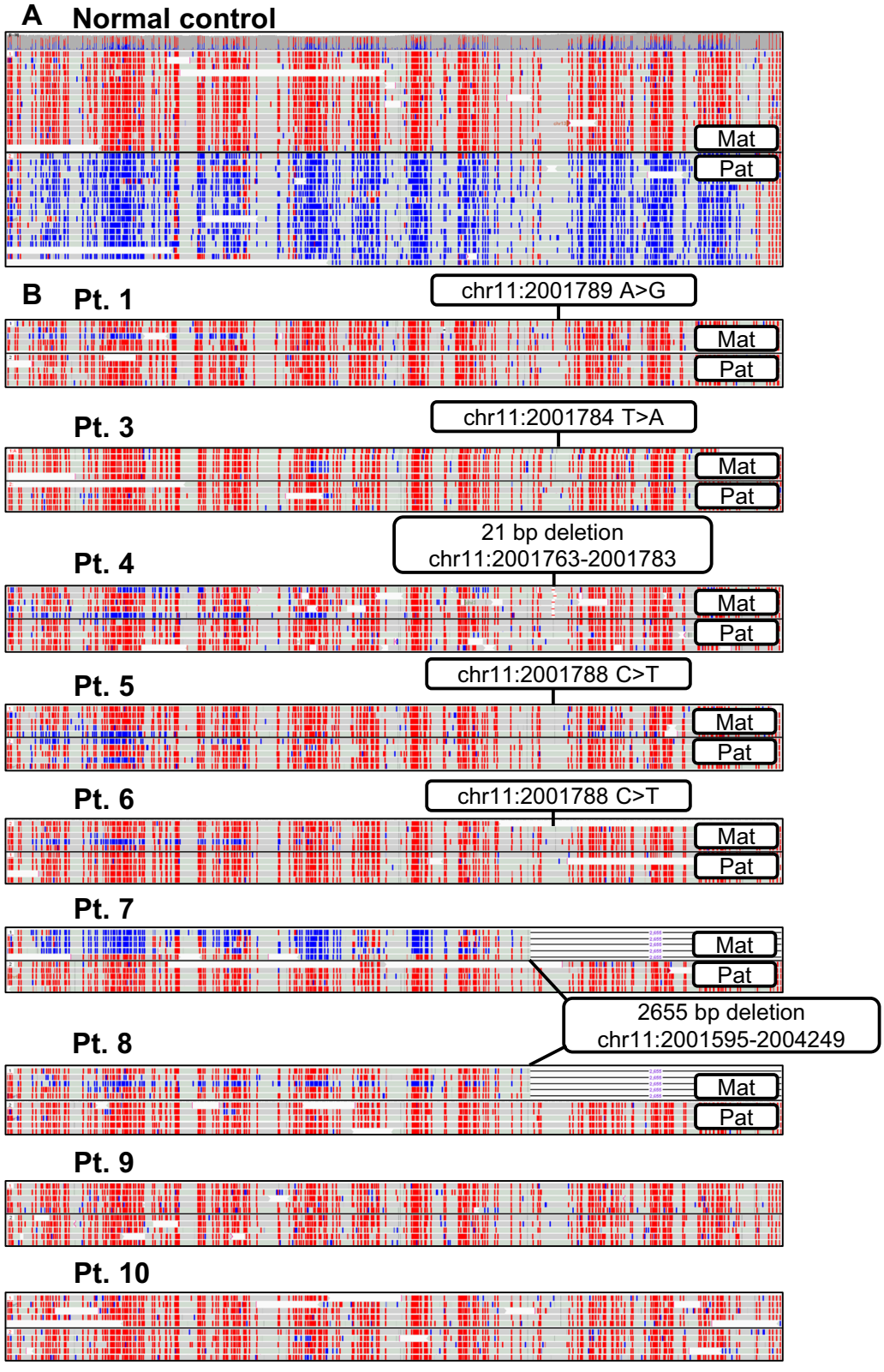

Fig. 4 The results of methylation analysis for the *H19*-DMR using LRS analysis on IGV. **A** The results of methylation analysis using LRS analysis on IGV in the normal control. **B** The results of methylation analysis using LRS analysis on IGV in seven patients with OBS abnormalities and two patients without OBS abnormalities. The red square indicates methylated CpGs, and the blue square indicates unmethylated CpGs. IG, intergenic; DMR, differentially methylated region; IGV, Integrative Genomics Viewer, Mat, maternal allele; Pat, paternal allele

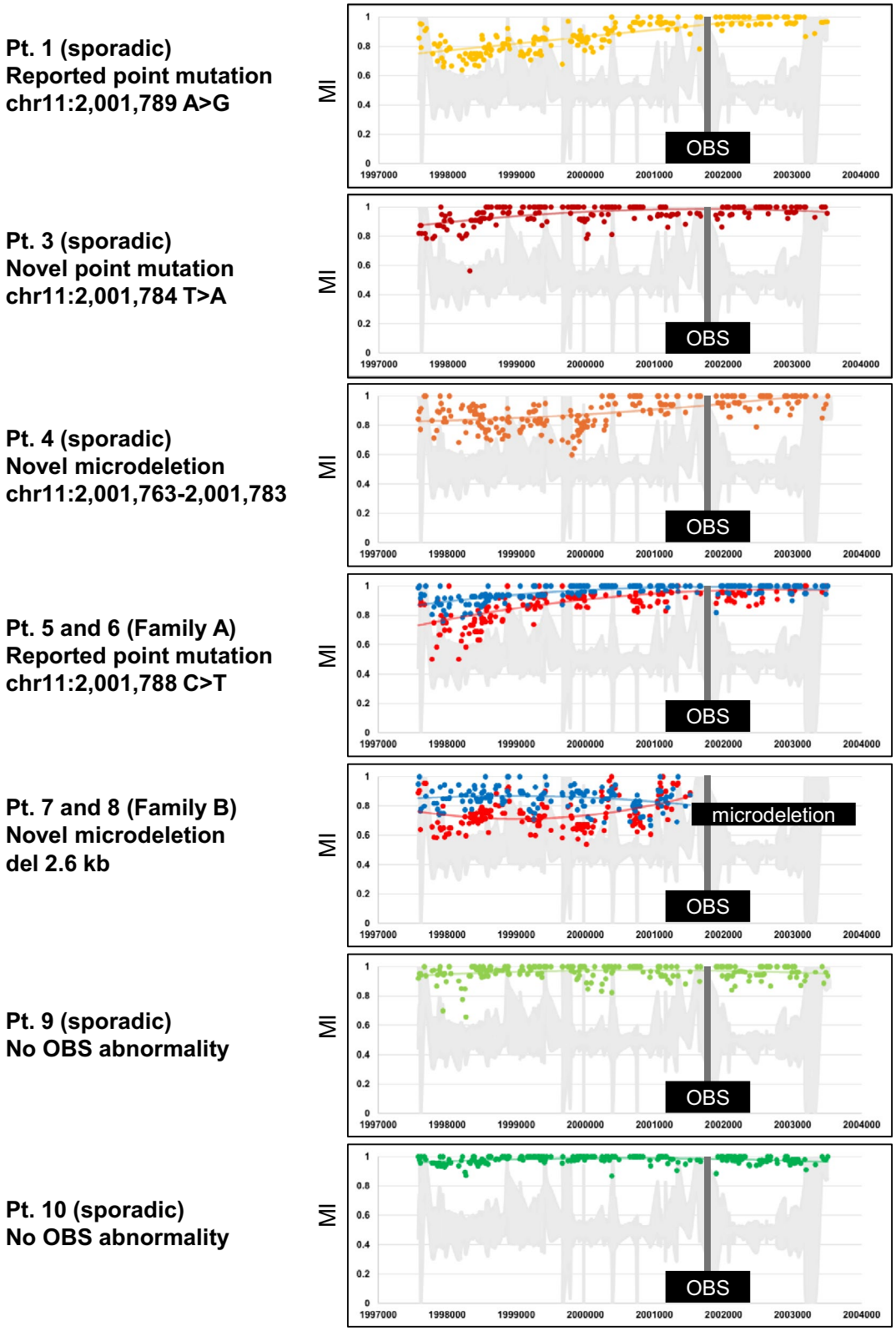

Fig. 5 MI plots of all CpGs within the *H19*-DMR in patients with various OBS abnormalities and without OBS abnormalities. A fitted curve is drawn for each patient. In Families A and B, the red points show the MIs of mothers, and the blue points show the MIs of the offspring. The gray background shows the normal range of MIs in CpGs. MI, methylation index; DMR, differentially methylated region; OBS, OCT4/SOX2 binding sites

Our study using T-LRS analysis first revealed continuous methylation levels of 247 CpGs within the *H19*-DMR in BWS patients with hypermethylation of the *H19*-DMR and identified differences in the methylation pattern between patients with various OBS abnormalities and patients without OBS abnormalities. As shown in Fig. 6, several studies showed methylation levels for CpGs in mainly CTCF-target-sites (CTS) in the *H19*-DMR using Southern blot hybridization analysis, bisulfite sequencing, and combined bisulfite restriction analysis in patients with microdeletions involving OBS [26–29] and patients with point mutations in OBS [9, 10, 20, 22]. In previous studies, cases with point mutations showed more severe hypermethylation, particularly at loci distant from the OBS, compared to cases with microdeletions (Fig. 6). Our patients with point mutations (Pt. 1, 3, 5 and 6) and a patient with a 21-bp deletion affecting OBS (Pt. 4) exhibited similar methylation patterns to those observed in previously reported cases with point mutations. Besides, OBS, including eight bases, is separated into two sites, namely ATTA (POU-S binding site) and GCAT (POU-HD binding site) [30]. Of our patients with OBS point mutations, Pt. 1, 5, and 6 had point mutations in the POU-HD binding site, and Pt. 3 and 4 had point mutations and microdeletions in the POU-S binding site. We compared MI plots between the group comprising patients 1, 5, and 6 and the group comprising patients 3 and 4, and no obvious differences were observed. It has been reported that the methylation status of CpG sites in OBS may affect the binding of OCT4/SOX2 [30]; however, OBS1 does not contain CpG sites. Therefore, differences in the position of point mutations within the POU-HD or POU-S binding sites in OBS1 may not affect the methylation pattern in the *H19*-DMR. However, Pt. 7 and 8 in family B with a microdeletion involving OBS showed different abnormal methylation patterns characterized by consistently moderate hypermethylation in whole CpGs in the *H19*-DMR. The *H19*-DMR has three OBS, including three octamer motifs (Fig. 6). We hypothesized two pathogenic mechanisms leading to this methylation pattern. First, in family B, OBS1 was deleted, but OBS0 was present in the nearest position where OBS1 should be. OBS0 may function similarly to OBS1, although a point mutation in OBS0 has not been reported in patients with hypermethylated *H19*-DMR. Second, a previous study reported that microdeletions that narrow the distance between CTSs cause severe methylation defects, whereas the microdeletions involving CTSs cause mild methylation defects [31]. As shown in Fig. 6, the microdeletion in Family B deleted three CTSs, and the methylation defect pattern was mild compared with that in patients with point mutations. On the other hand, the microdeletion in Pt. 4 affected only one base of OBS and did not involve CTSs. Therefore, the OBS abnormality in Pt. 4 may have caused methylation defects.

In both families A and B, methylation levels of CpGs in the *H19*-DMR were higher in offspring than in mothers. Recently, it has been reported that SOX2 binding to OBS maintains unmethylation of CpGs by inhibiting DNMT1-dependent methylation, and this effect is further enhanced by co-binding with OCT4 [32]. After the elimination of parental imprints, such as DNA methylation, in the embryo's primordial germ cells (PGC), the CpGs in the *H19*-DMR are methylated during spermatogenesis and remain unmethylated during oogenesis [33]. The methylation pattern of the *H19*-DMR, which is methylated CpGs on the paternal allele and unmethylated CpGs on the maternal allele, is maintained after fertilization [33]. Although the pathogenic mechanism, in which OBS abnormalities lead to hypermethylation of the *H19*-DMR, remains to be elucidated in detail, we hypothesize that the elimination of abnormal methylation at the *H19*-DMR in PGCs in oocytes from mothers with OBS abnormalities may be insufficient, resulting in a more hypermethylated *H19*-DMR in the offspring. Further studies in this field will clarify these matters.

Our study detected no significant differences in clinical symptoms between patients with and without OBS abnormalities. Furthermore, differences in MIs of CpGs in the *H19*-DMR between mothers and their offspring did not correlate with clinical symptoms. Although the presence or absence of DNA methylation abnormalities in the disease-responsible DMR appears to be important for clinical manifestation, the aberrant methylation levels in themselves may have a limited impact on symptom development. Further accumulation of cases is necessary to clarify the relationship between methylation abnormalities and clinical symptoms.

As shown in Fig. 3, in the *H19*-DMR, many CpGs had MIs around 0.5 (imprinted), but some CpGs showed MIs over 0.8 (not imprinted), as previously reported [24]. Furthermore, according to previous reports, we set the lower limit on the number of reads to 12, but the number of reads affects methylation analysis using LRS. In future clinical LRS-based genetic testing, selecting imprinted CpGs, obtaining additional control samples, and obtaining further reads would be needed to define the normal range.

Conclusion

We identified OBS abnormalities in approximately 30% of sporadic BWS patients with hypermethylation of the *H19*-DMR. Genetic examination for OBS should be considered in patients with BWS showing hypermethylated *H19*-DMR. T-LRS analysis for the *H19*-DMR revealed differences in the methylation patterns with or without OBS abnormalities and in the methylation levels of each

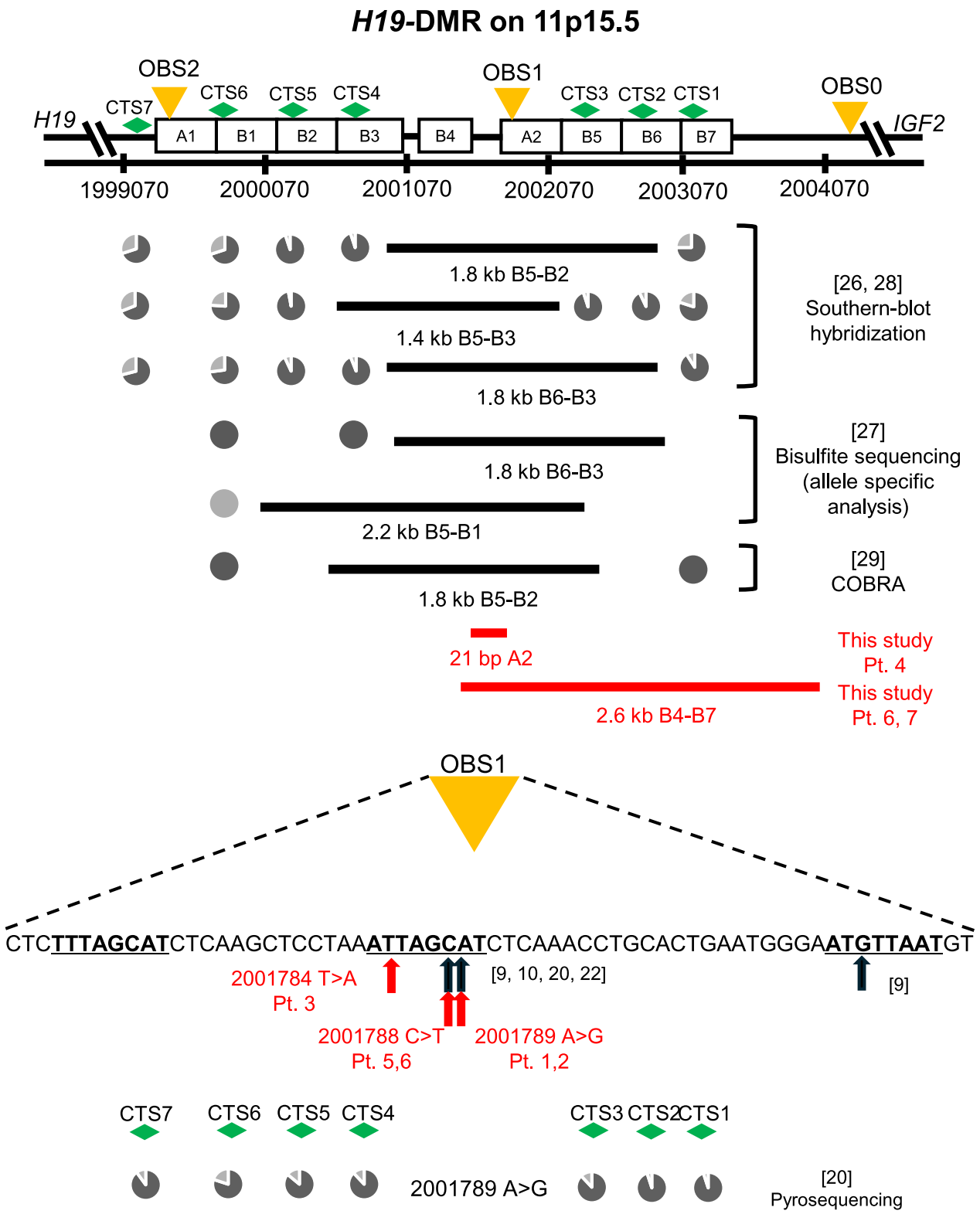

Fig. 6 Schematic diagram of the *H19*-DMR, OBS abnormalities in previous studies and our study, and the results of methylation analysis in previous studies. A. Diagram of the *H19*-DMR, deleted regions in cases, and the results of methylation analysis. B. The sequence of OBS1, point mutations on OBS1 in reported cases and our patients, and the results of methylation analysis. The pie chart shows the methylation levels in CpG sites from the previous studies. The dark gray in the pie chart indicates the methylation ratio in the examined CpGs. Black bars and characters show the previously reported cases and deleted sizes in these cases. The red bar and characters show the OBS abnormalities in our patients. Underlined sequences in OBS1 are the OCT4/SOX2 binding motif. DMR, differentially methylated region; OBS, OCT4/SOX2 binding site; CTS, CTCF target site; A, repeat block A; B, repeat block B; COBRA, combined bisulfite restriction analysis

CpG between mothers and their offspring with the same OBS abnormalities.

Methods

This study was approved by the Institutional Review Board Committee at the National Center for Child Health and Development.

Identification of hypermethylation of the H19-DMR

We conducted methylation analysis using pyrosequencing as previously reported [16–18] and/or MS-MLPA analysis according to the manufacturer's protocol in 233 patients suspected of having BWS. Genetic testing for BWS detected 18 patients with epimutation showing only hypermethylated *H19*-DMR, 45 patients with epimutation showing only hypomethylated *Kv*-DMR, 40 patients with UPD(11)pat, two patients with pathogenic variants in *CDKN1C,* six patients with MLID, and 122 patients with unknown etiologies or other diseases. Patients other than those with epimutation showing only hypermethylated *H19*-DMR were excluded from this study.

Clinical characteristics of the patients

We obtained clinical features of patients with hypermethylated *H19*-DMR using a questionnaire from their attending physicians.

Sample preparation

We obtained genomic DNA from leukocytes of patients and controls with the Monarch HMW DNA Extraction Kit for Cells & Blood (New England Biolabs) or the Gentra Puregene Blood Kit (Qiagen) according to the manufacturer's instructions.

Amplicon sequencing analysis for the H19-DMR

We conducted amplicon sequencing, as previously reported [19]. In brief, we amplified a region of approximately 9 kb with the primer set shown in Table S4. For library preparation, we used the NEBNext Ultra II FS DNA Library Prep Kit for Illumina (Illumina) with the PCR product targeted to the entire *H19*-DMR, following the manufacturer's protocol. The libraries were subjected to MiSeq (Illumina) and sequenced to identify abnormalities in OBS.

Sanger sequencing

To confirm OBS abnormalities detected by amplicon sequencing, we conducted Sanger sequencing in patients with OBS abnormalities and their family members. Furthermore, to evaluate the parental origin of the alleles with the mutations detected in mothers without BWS-like phenotypes, we conducted Sanger sequencing with genomic DNA treated with AccII, which is MSRE. The primer sets used in the Sanger sequencing are shown in Table S4.

T-LRS analysis

For LRS analysis, we applied adaptive sampling to enrich reads. We designed targeted regions for 24 DMRs related to imprinting disorders and 48 DMRs with unknown effects on imprinting disorders, based on previous studies [8, 23], and genes associated with imprinting disorders in the BED file as targeted regions (Table S2), and the targeted regions comprising 1.2% of the whole genome.

For library preparation, we conducted fragmentation of DNA samples (2–4 μg) from patients and controls using g-TUBE (Covaris) and removed small molecules using Short Read Eliminator (PacBio) to obtain high-quality data. Subsequently, we created libraries using the Ligation Sequencing Kit V14 (ONT) and the NEB Next Companion Module for Oxford Nanopore Technologies Ligation Sequencing (ONT). The prepared libraries were subjected to MinION or PromethION flow cells (R10.4.1) and sequenced the libraries with the GridION Mk1 or PromethION 2 solo (ONT) device under MinKNOW v22.12.5 or v23.11.7 (ONT) control. We washed the flow cell with the Flow Cell Wash Kit and reloaded the library twice during sequencing (at 18 h and 42 h). The sequence data was output in POD5 file format. We used Guppy 6.4.6 (dna_r10.4.1_e8.2_400bps_modbases_5mc_cg_hac.cfg), which is the official ONT basecaller to create BAM files containing mapping and methylation information, and PEPPER-Margin Deep Variant (pepper_deepvariant_r0.8-gpu.sif) for haplotyping and allele-specific analysis. We visualized the BAM files on the IGV. We first could not obtain the aligned reads for the *H19*-DMR due to multiple hits. After excluding the chr11_KI270721v1_random sequence from the reference FASTA file (GRCh38 with decoy), we obtained the reads aligned to the *H19*-DMR. We calculated MIs for all CpGs on each haplotype and total using Modkit (https://github.com/nanoporetech/modkit). We uploaded the script for bioinformatic analysis to Dryad (https://doi.org/10.5281/zenodo.17933283).

Definition of the normal range of methylation indexes for CpGs in the H19-DMR by LRS analysis

We defined the region as the *H19*-DMR based on previous studies [8, 23], which included 247 CpGs. To define the normal range for MIs of 247 CpGs within the *H19*-DMR, we conducted LRS in seven healthy controls. We calculated the MI (ranging from 0 to 1) of a CpG by adding the MI of the neighboring sense and antisense strands in normal controls with Modkit. Modkit produces the MI by dividing the number of reads having methylated CpGs by the total number of reads having unmethylated CpGs and methylated CpGs for each haplotype. CpGs with 0.3

or less probability of 5mC were classified as unmethylated CpGs, and CpGs with 0.7 or more probability of 5mC were classified as methylated CpGs. We defined the normal range of MI for each CpG as $|MI| < 3$ SD in seven healthy controls.

Statistical analysis

The statistical significance of the median and frequency of clinical data obtained from patients with OBS abnormalities and patients without OBS abnormalities were examined using the Mann–Whitney U test and Fisher's exact probability test, respectively. $P < 0.05$ was considered significant.

Abbreviations

BWS	Beckwith-Wiedemann syndrome
BWSp	BWS spectrum
DMR	Differentially methylated region
H19	*H19/IGF2*:IG
Kv	*KCNQ1OT1*
OBS	OCT4/SOX2 binding site
CTS	CTCF target site
LRS	Long-read sequencing
TLRS	Targeted LRS
ONT	Oxford nanopore technologies
MS-MLPA	Methylation-specific multiple ligation-dependent probe amplification
PGC	Primordial germ cells
IGV	Integrative genomics viewer
MI	Methylation index

Supplementary Information

The online version contains supplementary material available at https://doi.org/10.1186/s13148-026-02065-5.

Additional file1 (PPTX 5011 KB)

Additional file2 (PPTX 923 KB)

Additional file3 (PPTX 177 KB)

Additional file4 (XLSX 62 KB)

Additional file5 (XLSX 17 KB)

Additional file6 (XLSX 31 KB)

Additional file7 (XLSX 12 KB)

Acknowledgements

We are grateful to all patients and their parents for their cooperation. We thank Prof. Satoshi Narumi for his support throughout this research. We also thank Ms. Aki Ueda and Ms. Saori Miyasako for their support in molecular and data analysis.

Author contributions

HM designed the project, performed the molecular and data analyses, and wrote the paper. TU performed the molecular and data analysis. RK, RN, YW, SD, HY, RK, YN, HS, and TO obtained clinical information. MF reviewed the paper. MK designed the project, wrote and reviewed the paper, supervised the project, and gave final approval for the publication of this version. All authors read and approved of the final manuscript.

Funding

This work was supported by grants from the National Center for Child Health and Development (2022B-5), the Japan Society for the Promotion of Science (JSPS) (22K07858 [C]), the Japan Agency for Medical Research and Development (AMED) (23ek0109672, 23ek0109674, 24ek0109587, 24K02422 and JP25ek0109805), the NOVARTIS Foundation (Japan), and Kawano Masanori Memorial Public Interest Incorporated Foundation for Promotion of Pediatrics.

Data availability

Although we did not extract specific regions for analysis in this study, we uploaded our datasets, which extracted all relevant raw data for the *H19* -DMR across all patients and controls, in BAM format, as supplementary information.

Declarations

Ethics approval and consent to participate

This study was reviewed and approved by the Institutional Review Board Committee at the National Center for Child Health and Development (518) and was in accordance with the Declaration of Helsinki.

Consent for publication

We obtained written informed consent from the patients or the patients' parents to publish patients' clinical and molecular information.

Competing interests

The authors declare no competing interests.

Author details

[1]Department of Molecular Endocrinology, National Research Institute for Child Health and Development, 2-10-1 aOkura, Setagaya-Ku, Tokyo 157-8535, Japan
[2]Department of Pediatrics, Keio University School of Medicine, 35 Shinanomachi, Shinjuku-Ku, Tokyo 160-8582, Japan
[3]Department of Pediatrics, Nagasaki University Graduate School of Biomedical Sciences, 1-7-1, Sakamoto, Nagasaki 852-8501, Japan
[4]Division of Medical Genetics, National Center for Child Health and Development, 2-10-1 Okura, Setagaya-Ku, Tokyo 157-8535, Japan
[5]Department of Pediatrics, Tokyo University, 7-3-1, Hongo, Bunkyo-Ku, Tokyo 113-8655, Japan
[6]Department of Pediatrics, Jichi Medical University, 3311-1, Yakushiji, Shimotsuke 329-0498, Japan
[7]Department of Pediatrics, Iwate Medical University, 2-1-1, Idaidori, Yahaba 028-3695, Japan
[8]Department of Pediatrics, University of Yamanashi, 1110, Shimokato, Chuo 409-3898, Japan
[9]Department of Pediatrics, Hiroshima University Graduate School of Biomedical and Health Sciences, 1-2-3, Kasumi, Minami-Ku, Hiroshima 734-8551, Japan
[10]Department of Neonatology, Hiroshima City Hiroshima Citizens Hospital, 7-33 Motomachi, Naka-Ku, Hiroshima 730-8518, Japan
[11]Department of Biomolecular Sciences, Faculty of Medicine, Saga University, 5-1-1 Nabeshima, Saga 849-8501, Japan
[12]Department of Pediatrics, Hamamatsu Medical Center, 328 Tomizuka-Cho, Chuo-Ku, Hamamatsu 432-8580, Japan
[13]Department of Biochemistry, Hamamatsu University School of Medicine, 1-20-1 Handayama, Chuo-Ku, Hamamatsu 431-3192, Japan

Received: 14 July 2025 / Accepted: 21 January 2026
Published online: 03 February 2026

References

1. Brioude F, Kalish JM, Mussa A, Foster AC, Bliek J, Ferrero GB, et al. Clinical and molecular diagnosis, screening and management of Beckwith–Wiedemann syndrome: an international consensus statement. Nat Rev Endocrinol. 2018;14(4):229–49. https://doi.org/10.1038/nrendo.2017.166.
2. Choufani S, Shuman C, Wakesberg R. Beckwith-Wiedemann syndrome. Am J Med Genet C Semin Med Genet. 2010;154C(3):343–54. https://doi.org/10.1002/ajmg.c.30267.
3. Cooper WN, Luharia A, Evans GA, Raza H, Haire AC, Grundy R, et al. Molecular subtypes and phenotypic expression of Beckwith-Wiedemann syndrome. Eur J Hum Genet. 2005;13(9):1025–32. https://doi.org/10.1038/sj.ejhg.5201463.

4. Papulino C, Chianese U, Nicoletti MM, Benedetti R, Altucci L. Preclinical and clinical epigenetic-based reconsideration of Beckwith-Wiedemann syndrome. Front Genet. 2020;11:563718. https://doi.org/10.3389/fgene.2020.563718.
5. Eggermann T, Algar E, Lapunzina P, Mackay D, Maher ER, Mannens M, et al. Clinical utility gene card for Beckwith-Wiedemann syndrome. Eur J Hum Genet. 2014;22(3):7–10. https://doi.org/10.1038/ejhg.2013.132.
6. Chiesa N, Cresceenzo AD, Mishra K, Perone L, Carella M, Palumbo O, et al. The KCNQ1OT1 imprinting control region and non-coding RNA: new properties derived from the study of Beckwith-Wiedemann syndrome and Sliver-Russell syndrome cases. Hum Mol Genet. 2012;21(1):10–25. https://doi.org/10.1093/hmg/ddr419.
7. Zimmermann DL, Boddy CS, Schoenherr CS. Oct4/Sox2 binding sites contributed to maintaining hypomethylation of the maternal *Igf2/H19* imprinting control region. PLoS ONE. 2013;8(12):e81962s.
8. Monk D, Morales J, Dunnen JT, Russo S, Court F, Prawitt D, et al. Recommendations for a nomenclature system for reporting methylation aberrations in imprinted domains. Epigenetics. 2018;13(2):117–21. https://doi.org/10.1080/15592294.2016.1264561.
9. Higashimoto K, Jozaki K, Kosho T, Matsubara K, Fuke T, Yamada D, et al. A novel de novo point mutation of the OCT-binding site in the *IGF2/H19*-imprinting control region in Beckwith-Wiedemann syndrome patient. Clin Genet. 2014;86(4):539–44. https://doi.org/10.1111/cge.12318.
10. Abi Habib W, Azzi S, Brioude F, Steunou V, Thibaud N, Das Neves C, et al. Extensive investigations of the *IGF2/H19* imprinting control region reveals novel OCT4/SOX2 binding site defects associated with specific methylation patterns in Beckwith-Wiedemann syndrome. Hum Mol Genet. 2014;23(21):5763–73. https://doi.org/10.1093/hmg/ddu290.
11. Ashton PM, Nair S, Dallman T, Rubino S, Rabsch W, Mwaigwisya S. MinION nanopore sequencing identifies the position and structure of a bacterial antibiotic resistance island. Nat Biotechnol. 2015;33(3):296–300. https://doi.org/10.1038/nbt.3103.
12. Laver T, Harrison J, O'Neill PA, Moore K, Farbos A, Paszkiewicz K, et al. Assessing the performance of the Oxford Nanopore Technologies MinION. Biomol Detect Quantif. 2015;3:1–8. https://doi.org/10.1016/j.bdq.2015.02.001.
13. Sigurpalsdottir BD, Stefansson OA, Holley G, Beyter D, Zink F, Hardarson MP, et al. A comparison of methods for detecting DNA methylation from long-read sequencing of human genomes. Gen Biol. 2024;25(1):69. https://doi.org/10.1186/s13059-024-03207-9.
14. Martin S, Heavens D, Lan Y, Horsfield CMD, Leggett RM. Nanopore adaptive sampling: a tool for enrichment of low abundance species in metagenomic samples. Genome Biol. 2022;23(1):11. https://doi.org/10.1186/s13059-021-02582-x.
15. Berivan B, Sanaa C, Yi C, Cheryl S, Nicole P, Emmanuelle L, et al. High frequency of copy number variations (CNVs) in the chromosome 11p15 region in patients with Beckwith-Wiedemann syndrome. Hum Genet. 2013;133(3):321–30. https://doi.org/10.1007/s00439-013-1379-z.
16. Fuke T, Mizuno S, Nagai T, Hasegawa T, Horikawa R, Miyoshi Y, et al. Molecular and clinical studies in 138 Japanese patients with Silver-Russell syndrome. PLoS One. 2013;8(3):e60105. https://doi.org/10.1371/journal.pone.0060105.
17. Kagami M, Mizuno S, Matsubara K, Nakabayashi K, Sano S, Fuke T, et al. Epimutations of the IG-DMR and the MEG3-DMR at the 14q32.2 imprinted region in two patients with Silver–Russell Syndrome-compatible phenotype. Eur J Hum Genet. 2015;23(8):1062–7. https://doi.org/10.1038/ejhg.2014.234.
18. Kagami M, Yanagisawa A, Ota M, Matsuoka K, Nakamura A, Matsubara K, et al. Temple syndrome in a patient with variably methylated CpGs at the primary MEG3/DLK1:IG-DMR and severely hypomethylated CpGs at the secondary MEG3:TSS-DMR. Clin Epigenet. 2019;11(1):42. https://doi.org/10.1186/s13148-019-0640-2.
19. Uehara E, Abe K, Nakao K, Muroya K, Hattori A, Matsubara K, et al. Molecular and clinical features of congenital hypothyroidism due to multiplex DUOX2 variants. Thyroid. 2024;34(7):827–36. https://doi.org/10.1089/thy.2024.0046.
20. Sun F, Higashimoto K, Awaji A, Ohishi K, Nishizaki N, Tanoue Y, et al. The extent of DNA methylation anticipation due to a genetic defect in ICR1 in Beckwith-Wiedemann syndrome. J Hum Genet. 2019;64(9):937–43.
21. Masunaga Y, Inoue T, Yamoto K, Fujisawa Y, Sato Y, Sonoyama Y, et al. IGF2 mutations. J Clin Endocrinol Metab. 2020;105(1):dgz034.
22. Demars J, Shmela ME, Rossignol S, Okabe J, Netchine I, Azzi S, et al. Analysis of the *IGF2/H19* imprinting control region uncovers new genetic defects, including mutations of OCT-binding sequences, in patients with 11p15 fetal growth disorders. Hum Mol Genet. 2010;19(5):803–14.
23. Joshi RS, Garg P, Zaitlen N, Lappalainen T, Watson CT, Azam N, et al. DNA methylation profiling of uniparental disomy subjects provides a map of parental epigenetic bias in the human genome. Am J Hum Genet. 2016;99(3):555–66. https://doi.org/10.1016/j.ajhg.2016.06.032.
24. Baekgaard CH, Lester EB, Larsen SM, Lauridsen MF, Larsen MJ. Nanoimprint: a DNA methylation tool for clinical interpretation and diagnosis of common imprinting disorders using nanopore long-read sequencing. Ann Hum Genet. 2024;88(5):392–8.
25. Urakawa T, Hattori A, Ogiwara Y, Masubuchi H, Igarashi M, Nakamura S, Hara-Isono K, Ishiwata K, Ogata-Kawata H, Kamura H, Kuroki Y, Nakabayashi K, Fukami M, Kagami M. A comprehensive long-read sequencing system to assess DNA methylation at differentially methylated regions and imprinting-disorder-related genes. Genome Med. 2025;17(1):144. https://doi.org/10.1186/s13073-025-01559-w
26. Sparago A, Russo S, Cerrato F, Ferraiuolo S, Castorina P, Selicorni A, et al. Mechanisms causing imprinting defects in familial Beckwith–Wiedemann syndrome with Wilms' tumour. Hum Mol Genet. 2007;16(3):254–64. https://doi.org/10.1093/hmg/ddl448.
27. Prawitt D, Enklaar T, Rupprecht BG, Spangenberg C, Oswald M, Lausch E, et al. Microdeletion of target sites for insulator protein CTCF in a chromosome 11p15 imprinting center in Beckwith-Wiedemann syndrome and Wilm's tumor. Proc Natl Acad Sci. 2005;102(11):4085–90. https://doi.org/10.1073/pnas.0500037102.
28. Sparago A, Cerrato F, Vernucci M, Ferrero GB, Silengo MC, Riccio A. Microdeletions in the human H19 DMR result in loss of IGF2 imprinting and Beckwith-Wiedemann syndrome. Nat Genet. 2004;36(9):958–60. https://doi.org/10.1038/ng1410.
29. Crescenzo AD, Coppola F, Falco P, Bernardo I, Ausanio G, Cerrato F, et al. A novel microdeletion in the *IGF2/H19* imprinting centre region defines a recurrent mutation mechanism in familial Beckwith-Wiedemann syndrome. Eur J Med Genet. 2011;54(4):e451–4. https://doi.org/10.1016/j.ejmg.2011.04.009.
30. Tan DS, Cheung SL, Gao Y, Weinbuch HuH, Shi L, et al. The homeodomain of Oct4 is a dimeric binder of methylated CpG elements. Nucleic Acid Res. 2023;51(3):1120–38.
31. Beygo J, Citro V, Sparago A, Crescenzo AD, Cerrato F, Heitmann M, et al. The molecular function and clinical phenotype of partial deletions of the *IGF2/H19* imprinting control region depends on the spatial arrangement of the remaining CTCF-binding sites. Hum Mol Genet. 2013;22(3):544–57. https://doi.org/10.1093/hmg/dds465.
32. Vanzan L, Soldati H, Ythier V, Anand S, Braun S, Francis N, et al. High throughput screening identifies SOX2 as a super pioneer factor that inhibits DNA methylation maintenance at its binding sites. Nat Commun. 2021;12(1):3337.
33. Guo F, Yan L, Guo H, Li L, Hu B, Zhao Y, et al. The transcriptome and DNA methylation landscapes of human primordial germ cells. Cell. 2015;161(6):1437–52. https://doi.org/10.1016/j.cell.2015.05.015.

Publisher's Note